

# Quantitative evaluation of mechanical characteristics of Al-Si cast alloys: A parametric study

\*Ahmed Osman<sup>1</sup>, Naser A. Alsaleh<sup>2</sup>, Mahmoud Ahmadein<sup>3</sup>, and Mahmoud A. El-Sayed<sup>4</sup>

1. Department of Marine and Offshore Engineering, Arab Academy for Science Technology and Maritime Transport, Alexandria 21599, Egypt

2. Industrial Engineering Department, Imam Mohammad Ibn Saud Islamic University (IMSIU), 11432 Riyadh, Saudi Arabia

3. Department of Production Engineering and Mechanical Design, Tanta University, Tanta 31512, Egypt

4. Department of Industrial and Management Engineering, Arab Academy for Science Technology and Maritime Transport, Alexandria 21599, Egypt

Copyright © 2026 Foundry Journal Agency

**Abstract:** A parametric study was performed to explore the effect of runner thickness, filtration, and hydrogen content on the mechanical properties and defect formation in Al-7%Si-0.3%Mg (2L99) sand castings. A two-level full factorial design of experiments was used to statistically evaluate these parameters and the tensile properties were characterized via Weibull distribution analysis. The findings reveal that decreasing the runner thickness from 25 mm to 10 mm and using 10 PPI ceramic filters improve mechanical properties by minimizing double oxide film entrapment as confirmed by electron microscopy examination. In addition, lowering hydrogen concentrations within the Al alloy from 0.24 cm<sup>3</sup>/100 g Al to 0.12 cm<sup>3</sup>/100 g Al is also shown to enhance casting integrity by suppressing bifilm inflation and subsequent pore formation. ANOVA results indicate that the hydrogen content is the most important factor, contributing 53% to the variability in mechanical properties, followed by filtration (25%) and runner thickness (17%). The optimized casting conditions including thin runners (10 mm thick), melt filtration, and a low hydrogen level (0.12 cm<sup>3</sup>/100 g Al), result in an approximately 474% increase in the shape factor and a 107% increase in the characteristic life of UTS, as well as an approximately 413% increase in the shape factor and a 149% increase in characteristic life of elongation. The outcomes suggest that controlled filling systems and melt treatment are critical for producing consistent, high integrity aluminum castings in industrial applications.

**Keywords:** aluminum-silicon alloy; casting; mechanical properties; defect formation

CLC numbers: TG146.21

Document code: A

Article ID: 1672-6421(2026)02-158-11

## 1 Introduction

Aluminum alloys are increasingly used in the automotive and aerospace industries during the past decades due to their superior combination of properties. The main benefit stems from their exceptional strength-to-weight ratio, which allows for lightweight structural components that maintain mechanical performance. The combination

of inherent flexibility and corrosion resistance makes these alloys highly valuable for weight-sensitive engineering applications that require both durability and fuel efficiency<sup>[1]</sup>. Such useful characteristics make Al alloys suitable for replacing heavier materials in many applications. However, the presence of structural defects adversely affects mechanical properties of aluminum alloys, thereby compromising their overall quality.

The high chemical reactivity of molten aluminum alloys results in formation of a surface oxide layer on exposed surfaces. The protective film shows rapid reformation kinetics upon disruption, with studies showing complete surface re-oxidation in milliseconds under typical casting conditions<sup>[2, 3]</sup>. This instantaneous re-passivation behavior significantly influences melt handling and casting processes. Although the surface oxide is harmless when undisturbed, routine casting

### \*Ahmed Osman

Ph. D., Associate Professor. A member of Sigma XI Society. He got his Ph. D. in Engineering from Swinburne University of Technology, Melbourne, Australia. His research interests primarily focus on corrosion engineering, acoustic emission, materials engineering, and marine and offshore engineering. He maintains active multinational research collaborations, particularly across Europe, Oceania, and the Asia-Pacific region.

E-mail: ahmed.osman@aast.edu

Received: 2025-07-10; Revised: 2025-09-15; Accepted: 2025-11-24

practice, such as turbulent pouring, can mechanically disrupt the liquid metal surface. Such disruptions lead to the folding inward of the oxide layer to create encapsulated air pockets that become submerged in the melt bulk. This entrainment process is one of the primary mechanisms responsible for defect formation in aluminum casting operations<sup>[4]</sup>. This folding produces a famed casting defect called a double oxide film or bifilm – essentially two facing oxide layers around a gap of air. Bifilms are prior cracks within the microstructure, gravely weakening mechanical properties. The lack of atomic bonding across the inner bifilm interface often leaves areas of preferred failure and significantly reduces the fracture resistance during loading<sup>[5, 6]</sup>, see Fig. 1.

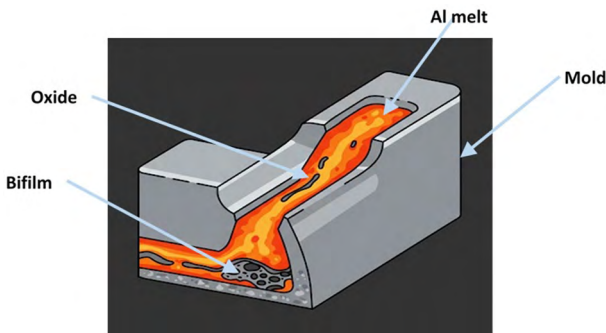


**Fig. 1: Formation and entrainment of double oxide film in aluminum castings**

Bifilms are also suggested to promote hydrogen porosity. Hydrogen has high solubility in molten aluminum but much lower solubility in solid aluminum. Therefore, during solidification, hydrogen is rejected from the solidifying metal and hence, would diffuse into the bifilm’s gas pocket, developing into a volumetric pore that further degrades mechanical properties<sup>[7, 8]</sup>. Recently, El-Sayed, Chen, and Griffiths et al. had quantitatively verified such mechanisms, demonstrating the formation of what could be called “bifilm-induced hydrogen porosity”, and its corresponding influence on mechanical properties<sup>[9-13]</sup>. Bifilms are therefore recognized by scientists as basic microstructural defects that negatively impact aluminum cast alloys in two ways: (1) by serving as the main stress crack initiator, and (2) by aiding in the nucleation of porosity. When these effects are combined, the material’s tensile strength and fatigue resistance are decreased, which causes the component to fail more quickly<sup>[14, 15]</sup>.

Bifilm entrainment occurs mainly during mold filling, with the critical velocity concept offering key insight into its origin. Critical velocity ( $V_c$ ) is described as the lowest possible melt velocity at which there would be enough surface turbulence to entrain oxide layers into the bulk liquid. In other words, the critical velocity refers to the highest allowable melt flow rate at the ingate, above which hydrodynamic pressures dominate surface tension forces, and surface oxide films become entrained in the bulk liquid<sup>[1]</sup>, and is estimated as below:

$$V_c = 2(\gamma \cdot g / \rho)^{1/4} \quad (1)$$

where  $\rho$  is the melt density in  $\text{kg} \cdot \text{m}^{-3}$ ,  $\gamma$  is the surface tension in  $\text{N} \cdot \text{m}^{-1}$  and  $g$  represents the gravitational acceleration in  $\text{m} \cdot \text{s}^{-2}$ .

For liquid aluminum  $\gamma=1 \text{ N} \cdot \text{m}^{-1}$  and  $\rho=2,400 \text{ kg} \cdot \text{m}^{-3}$ . Such material properties provide a threshold velocity of roughly  $0.5 \text{ m} \cdot \text{s}^{-1}$ . As the ingate velocity exceeds this value, inertial forces displace the melt surface, generating surface waves of sufficient amplitude that fold over and collapse under gravitational pull. This process captures the oxide layer within the liquid bulk and forms the typical bifilm defect structure that subsequently degrades the properties of the solidified casting<sup>[1, 14]</sup>. Investigations by Runyoro et al.<sup>[16]</sup>, Halvae and Campbell<sup>[17]</sup>, and Bahreinian et al.<sup>[18]</sup> across various aluminum and magnesium alloy systems indicated that the critical velocity typically falls within the range of  $0.4$  to  $0.6 \text{ m} \cdot \text{s}^{-1}$ . This narrow velocity window represents the transitional boundary between laminar and turbulent flow regimes that determine oxide film entrainment behavior in light alloy casting operations. The literature indicates that top-pouring practices generally fail to produce castings of acceptable quality. Studies suggest that melt integrity during filling can only be obtained by using customized bottom-pouring gating systems with a special design that could fulfill critical ingate-velocity prerequisites for sound castings<sup>[19, 20]</sup>.

Design of Experiments (DoE) is a statistical and optimization technique which deals with the organized scheduling and assessment of a singular system or complete system technological processes. It uses defined variable inputs and resulting output measurements to assist researchers in discovering relationships alongside calculating possible interrelationships among multiple input and output variables<sup>[21, 22]</sup>. This is especially helpful for complex systems, in which there is a large number of interdependent input factors influence the output information and/or quality of the system<sup>[23]</sup>. The approach enables several input parameters to be varied simultaneously, making it possible to measure their separate and collective effects on system outputs<sup>[24]</sup>. In contrast to stepwise methods testing a single factor in isolation, this simultaneous measurement could divulge significant interactions between parameters that might otherwise go unnoticed. Among experimental designs, full factorial designs (FFD) give the most exhaustive study by iterating through every combination of factor levels feasible<sup>[25-27]</sup>. The simplest experimental design for DoE is a 2-level full factorial experiment wherein each input factor is evaluated at two levels (typically denoted as low and high values). For  $k$  factors, this design requires  $2^k$  experimental runs<sup>[28]</sup>.

Mechanical characteristics of light alloys had been extensively addressed by many studies focusing the influence of different casting parameters on mechanical properties. However, a systematic study of the statistical significance of such parameters on the properties of Al-Si cast alloys has not been fully explored. The current research was carried out to cover the research gap and utilize statistical techniques by employing statistical methodologies, a full factorial DoE coupled with analysis of variance (ANOVA) to identify the significant casting process parameters and systematically evaluate their effects on the UTS and percentage elongation of Al-Si castings. In addition, the application of DoE not only

allowed to statistically assess the significance of the studied parameters, but also provided a sort of quantification of the weight of each parameter in impacting the studied process outputs through the calculation of the standardized effects and percent contribution of each factor. Finally, the methodology would allow the detection of potentially consequential interactions among factors, which are commonly disregarded by traditional experimental approaches.

The current research has applied a  $2^3$  full factorial design of three sand casting parameters: runner thickness, filter usage, and hydrogen content with two levels for each parameter. This results in eight full factorial experiments. The effect of these factors on the amount and size of bifilm defects, and by implication, on the properties of Al-Si alloy castings was studied. This approach might provide quantified information on the primary factors that affect quality and reproducibility of light alloy castings.

## 2 Experimental methods

This work investigated the gravity sand casting process of 2L99 aluminum alloy to provide data regarding the impact of three process parameters that were justifiably important: (1) runner thickness, (2) filtration, and (3) hydrogen content. Four mechanical response parameters were compared, which were the shape factor (Weibull modulus) and characteristic life (position parameter) of ultimate tensile strength (UTS) and percentage elongation. Design Expert software Version 7.0.0 (Stat-Ease Inc., Minneapolis, USA) was utilized for conducting DoE and ANOVA studies. Again, a  $2^3$  factorial design was endorsed to examine the main and interaction effects of the selected process parameters. Each parameter was altered over two values resulting in a total of 8 experiments with different combinations of the studied casting conditions.

Resin-bonded sand molds, as illustrated in Fig. 2, were prepared. Each mold can produce 10 tensile test bars of 100 mm long and 11 mm in diameter. The sand binder system consisted of two resin components: (1) polymer-polyols (35%–50% by weight in trimethylbenzene) and (2) diphenylmethane diisocyanate (60%–80% by weight in high-boiling aromatic solvent), each added at 0.6% relative to the sand weight. For each of the eight parametric combinations, twenty test bars (cast in two moulds) were prepared. A 12 kg batch of 2L99 alloy was induction-melted (Inductotherm, Droitwich, UK) for each condition, held at 800 °C under a partial vacuum of 0.2 bar for 2 h, a treatment which has been shown to remove any pre-existing oxide films<sup>[28, 29]</sup>. The melt was then poured at 700 °C from a height of 1 m above the mold pouring basin into the molds, intentionally generating surface turbulence to cause new double oxide film engendering and entrainment for controlled defect studies.

To evaluate the effect of hydrogen (H) content on casting quality, the experimental design included two distinct sets: a high-hydrogen group (Experiments 1–4) and a low-hydrogen group (Experiments 5–8). High-hydrogen castings were made

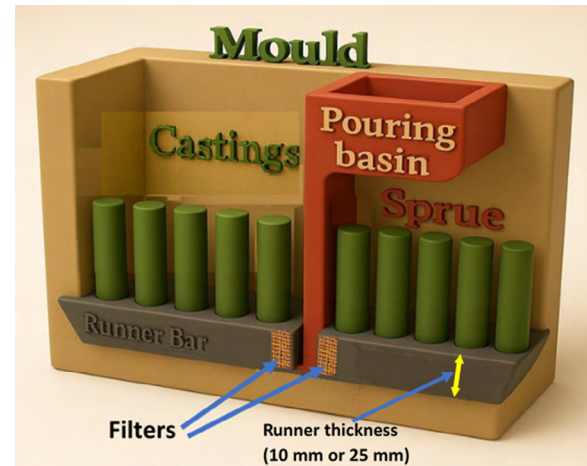


Fig. 2: Schematic illustration of the mold pattern design used for casting production

using sand moulds after aged at room temperature for 24 h before pouring, to remove surface moisture. The Al melt, after its initial 2 h holding under a partial vacuum of 0.2 bar at 800 °C, was poured into these molds immediately upon release from the vacuum chamber. On the other hand, for Experiments 5–8, in attempt to obtain castings with relatively lower hydrogen levels, the vacuum-treated melt was argon degassed at 750 °C for 1 h prior to pouring. Additionally, molds were pretreated under a vacuum of 500 mbar for two weeks to volatilize binder solvents and thus, minimize hydrogen pickup from the mold sand walls after pouring<sup>[29]</sup>.

In addition, the experimental setup employed two runner patterns with a thickness of 10 mm and 25 mm, respectively. Finally, to quantify the filtration impact, two ceramic filters (Fesoco, Birmingham, UK), with 10 pores per linear inch (PPI) and sizes of 50 mm×50 mm×20 mm, were positioned at the designated locations in the mold (see Fig. 2). The combined implementation of improved runner configuration and ceramic filtration is expected to improve the control over melt flow dynamics, thereby reducing oxide entrainment.

The solidified castings were then machined into tensile specimens of 37 mm in gauge length and 6.75 mm in diameter, with 20 test bars produced for each parametric combination. In addition, a sample was cut from the runner bar and its hydrogen content was analyzed using a LECO<sup>TM</sup> hydrogen analyzer (LECO, St. Joseph, MI, USA). The instrument operated using the inert gas fusion method, in which the sample was melted in a graphite crucible under a stream of inert carrier gas and the released hydrogen was quantified by thermal conductivity detection. The detection limit of the instrument is approximately 0.05 cm<sup>3</sup>/100 g Al, with an accuracy of ±0.01 cm<sup>3</sup>/100 g Al, ensuring reliable measurement of hydrogen levels in the cast samples. The mechanical test was conducted using the WDW-100E universal testing machine (Time Group Inc., Beijing, China) at a constant crosshead speed of 1 mm·min<sup>-1</sup>. The final ultimate tensile strength (UTS) and elongation values obtained were statistically compared using two-parameter Weibull analysis to quantify the variability in mechanical properties. Fractographic

examination was performed via a Philips XL-30 SEM (SEM Tech Solutions, North Billerica, USA) with EDX capability to demarcate bifilm-related fracture features.

### 3 Results

LECO analysis results revealed varying concentrations of hydrogen by experimental groups: the high-hydrogen samples (Experiments 1–4) averaged 0.24 cm<sup>3</sup>/100 g Al, while the low-hydrogen samples (Experiments 5–8) measured 0.12 cm<sup>3</sup>/100 g Al. This 50% reduction in hydrogen content resulted directly from the combined argon degassing treatment, applied to the melt at 750 °C, and extended mold vacuuming at 500 mbar for two weeks, which together minimize the hydrogen intensity both before and during solidification<sup>[30]</sup>.

The probability distributions of tensile properties (UTS and elongation) were statistically analyzed using EasyFit software (MathWave Technologies). As demonstrated in Fig. 3 for the UTS results from Experiment 2, the Weibull distribution fits significantly better than normal or exponential distributions. Such high correlation justified the use of Weibull analysis for characterizing the mechanical property data under all experimental conditions. Additional EasyFit analysis strictly confirmed the suitability of the Weibull distribution

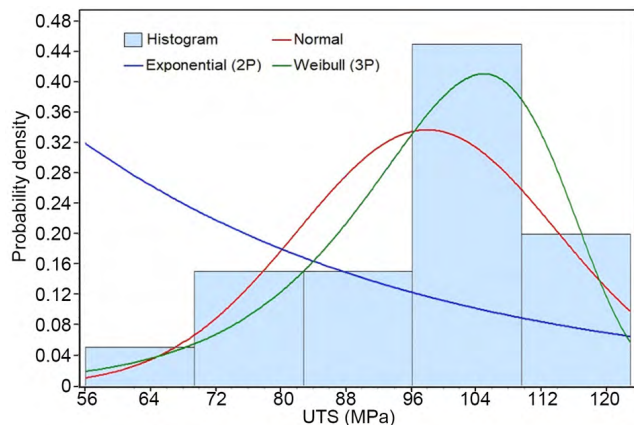


Fig. 3: UTS distribution for Experiment 2 test bars, demonstrating improved fit of Weibull distribution compared to other probability models

to all resulting property sets<sup>[31]</sup>. These findings would be a confirmation of earlier research results suggesting that the Weibull distribution would be preferable for representing the variation of properties of aluminum castings particularly for defect controlled failure mechanisms<sup>[32, 33]</sup>.

Hence, the two-parameter Weibull distribution was used in this research to characterize the mechanical properties of Al castings. The shape factor (or Weibull modulus) is a key measure of data scatter (uniformity) with the larger the value the smaller the data scatter<sup>[34]</sup>. Moreover, the characteristic life (or position parameter) is a threshold stress value at which about 37% of specimens are still functionally serviceable<sup>[35]</sup>. The shape factor and characteristic life are larger in castings with few defect populations, indicating superior mechanical properties and lower variation from piece to piece. This relationship arises from the inherent dependence of the statistical distribution of mechanical properties in cast alloys on its microstructural homogeneity. The Weibull parameters quantitatively reflect this relationship: defect-free microstructures yield higher average mechanical properties and reduced statistical scatter.

Figures 4(a)–(b) plot the Weibull distributions of UTS of specimens from high- and low-hydrogen environments, with corresponding elongation data being presented in Figs. 5(a)–(b). Strong linear correlations ( $R^2 > 0.9$ ) are found in all data sets, which confirms the applicability of the Weibull analysis. Notably, both UTS and elongation shape factors (trendline slopes) exhibit pronounced improvement in Experiments 5–8, where the hydrogen level was reduced by approximately 50% compared to high-hydrogen conditions.

Through the Weibull analysis, presented in Figs. 4 and 5, the shape factor and characteristic life of the UTS and elongation of castings under all experimental conditions were determined and summarized in Table 1. These four statistics were deemed as important response variables in the study.

It is shown that high-hydrogen castings (Experiments 1–4) possess the lowest UTS shape factor of 4.2 (25 mm runner, no filter), which improved to 6.6 (10 mm runner, no filter) and 7.8 (25 mm runner with filter). The optimum combination of a 10 mm runner and a filter achieves a shape factor of 18.4. Elongation shape factor shows an analogous trend, increasing

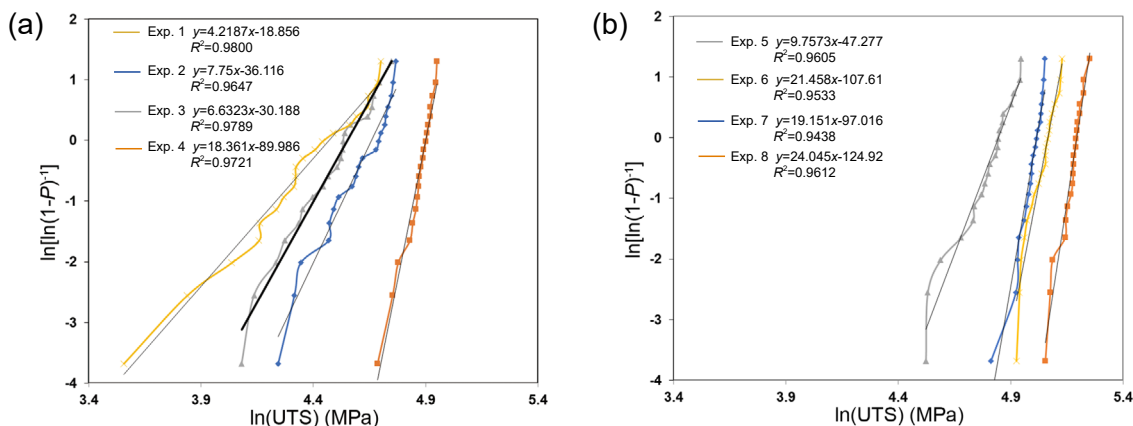


Fig. 4: UTS Weibull distributions for 2L99 alloy across experimental conditions: (a) Experiments 1 to 4; (b) Experiments 5 to 8

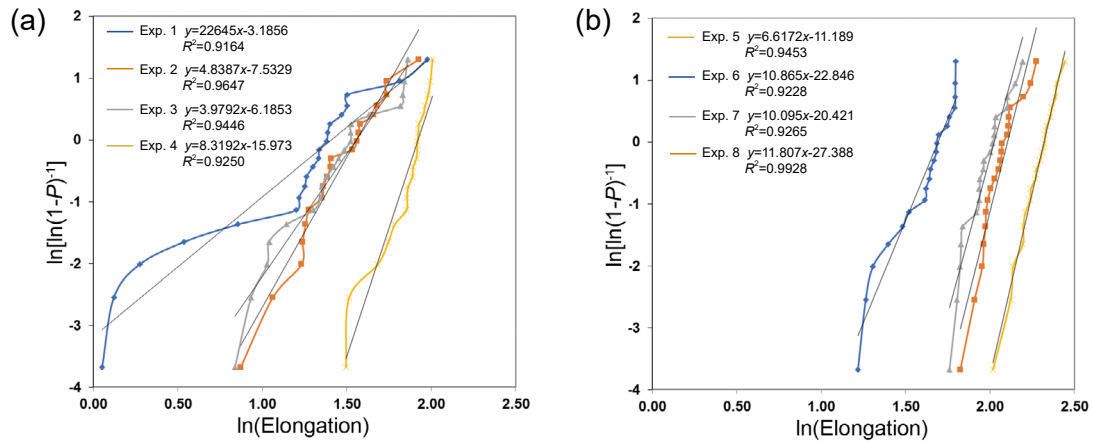


Fig. 5: Weibull distribution of elongation (%) for 2L99 alloy across experimental conditions: (a) Experiments 1 to 4; (b) Experiments 5 to 8

Table 1: Experimental design with corresponding Weibull statistics for UTS and elongation

Exp. No.	Casting conditions			UTS (MPa)		Elongation (%)	
	Runner thickness (mm)	Use of filters	Hydrogen content (cm <sup>3</sup> /100 g Al)	Shape factor	Characteristic life	Shape factor	Characteristic life
1	25	Unfiltered	0.24	4.2	87	2.3	4.1
2	25	Filtered	0.24	7.8	106	4.8	4.7
3	10	Unfiltered	0.24	6.6	95	4.0	4.7
4	10	Filtered	0.24	18.4	134	8.3	6.8
5	25	Unfiltered	0.12	9.8	127	6.6	5.4
6	25	Filtered	0.12	21.5	151	10.9	8.2
7	10	Unfiltered	0.12	19.2	158	10.1	7.6
8	10	Filtered	0.12	24.1	180	11.8	10.2

from 2.3 (lowest) to 8.3 (optimized conditions). Low-hydrogen castings (Experiments 5–8) demonstrate higher absolute values and significant relative improvements, with UTS shape factor rising from 9.8 to 24.1 and elongation shape factor from 6.6 to 11.8 as a result of the concurrent application of proper gating and filtration, signifying more reliable castings.

Both the UTS and elongation characteristic lives follow the trends of their shape factor. Implementing thin runners (10 mm) with filtration for low-hydrogen castings leads to the most significant gains, raising the UTS characteristic life from 127 to 180 MPa (42% improvement) and the elongation characteristic life from 5.4% to 10.2% (89% improvement). These gains, along with those associated with the shape factor, could be indicative of concerted improvements in both average properties (characteristic lives) and property consistency (shape factors) achieved through mould design optimization.

The results presented in Table 1 demonstrate that through employing the optimized conditions: low hydrogen level (0.12 cm<sup>3</sup>/100 g Al), with ceramic filtration, and thin runners (10 mm), mechanical properties of the castings as well as the property consistency, identified by means of characteristic lives and shape factors, respectively, can be remarkably enhanced. As can be inferred, the mechanical properties

reach peak characteristic life of 180 MPa for UTS and 10.2% for elongation, as well as the lowest property scatter (shape factors of 24.1 for UTS and 11.8% for elongation) when the proper casting parameters are applied (Experiment 8). This suggests that the mechanical improvement in both strength and reliability of Al-Si castings was achieved through coordinated process optimization.

The model adequacy was checked by using diagnostics: Normal probability plots of residuals (Fig. 6) show quite substantial linearity, and residual vs. run plots (Fig. 7) indicate random scatter around zero. This confirms the assumptions of normality and independence of residuals. These results reveal the robustness of the models, supporting their validity for further ANOVA-based significance testing.

The results presented in Table 1 were used as input to the DoE to perform the ANOVA statistical analysis. Model fitting analysis, using the least square method, was carried out to determine the best-fitted models that represent each of the studied responses (the shape factor and characteristic life of both the UTS and elongation) as a function of the studied parameters (runner thickness, filtration, and hydrogen content). Analysis of the fit summary output indicated that the best-fitted model is approximately linear for the four responses. The

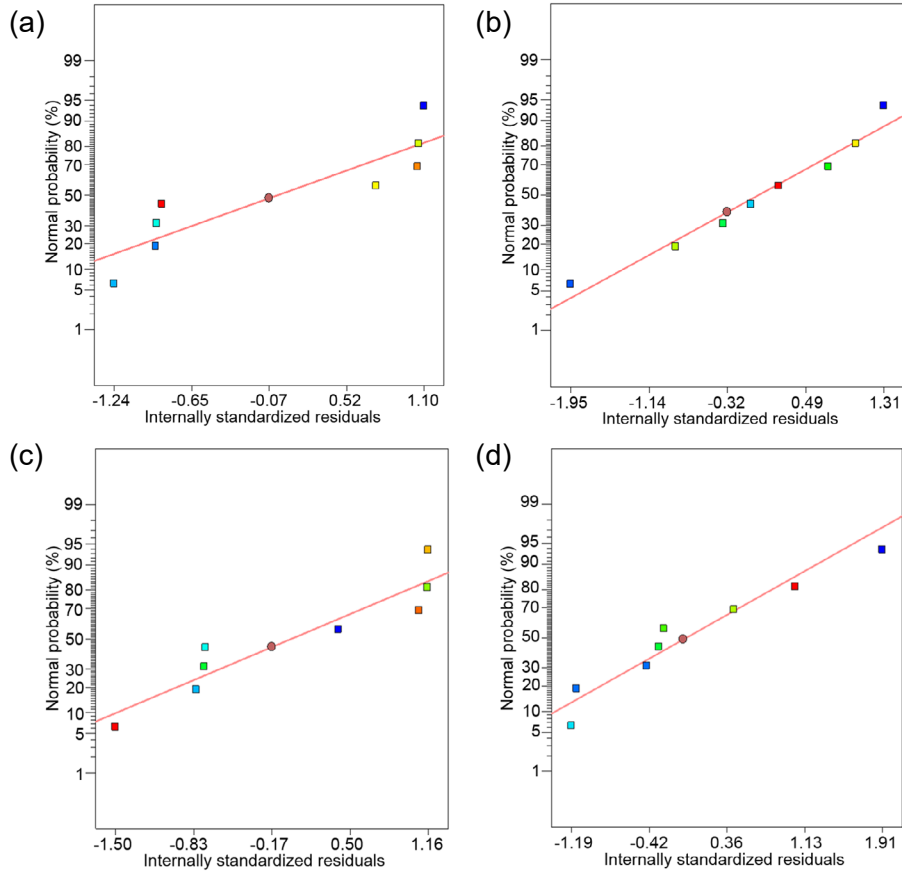


Fig. 6: Normal probability plots of residuals for UTS shape factor (a), UTS characteristic life (b), elongation shape factor (c), and elongation characteristic life (d), demonstrating conformance to linear model assumptions

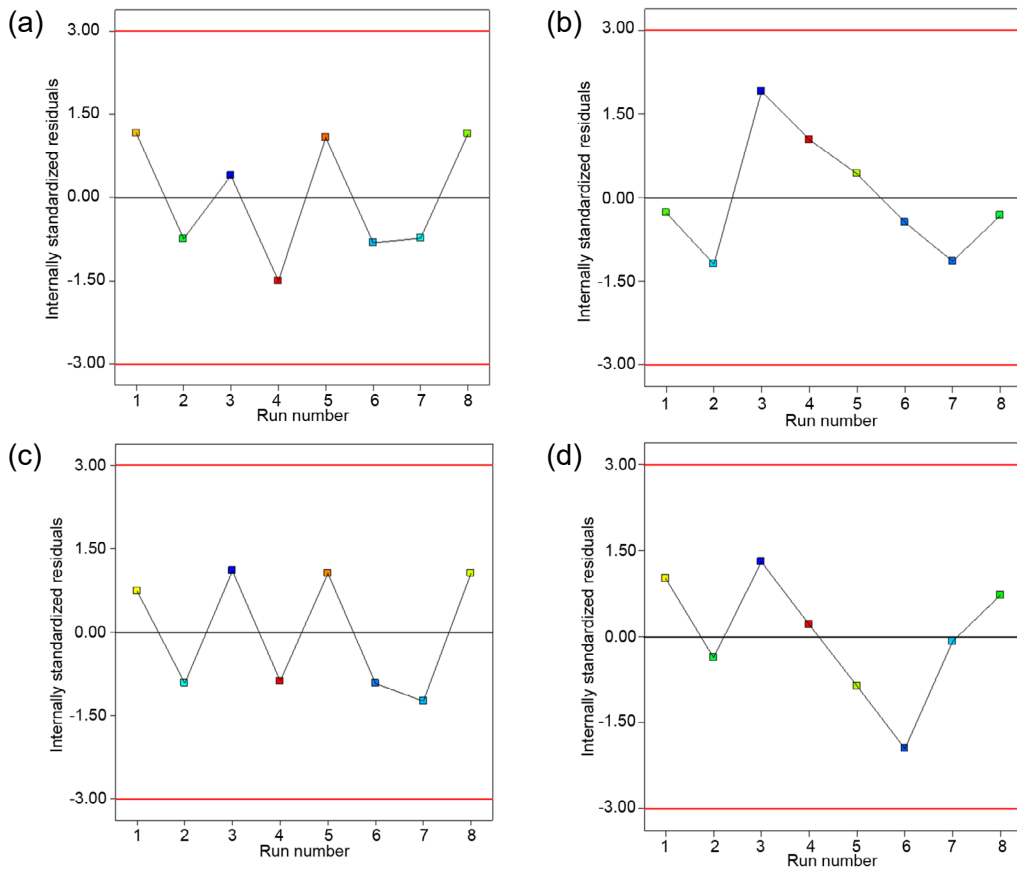


Fig. 7: Residual versus run plots for UTS shape factor (a), UTS characteristic life (b), elongation shape factor (c), and elongation characteristic life (d), confirming random error distribution and model validity

validated linear models quantified the effects of runner thickness, filtration, and hydrogen content on mechanical properties.

Table 2 presents the results of ANOVA, where *df* stands for degrees of freedom, and *F* represents the *F*-statistic value used to calculate the corresponding *p*-value. ANOVA determined the statistical significance (*p*-values) of the parameters and their interactions, and the standardized effects and percentage contributions ranked their importance. Again, the high *R*<sup>2</sup> values (0.93–0.97) and unbiased residuals confirmed that the models successfully captured the underlying process–property relationships for making strong conclusions about parameter effects. This approach not only identified critical factors but enabled optimization of the casting conditions for enhanced property magnitude (characteristic lives) and consistency (shape factors).

Statistical significance was assessed using *p*-values, and a value less than 0.05, corresponding to a 95% confidence level, indicates that the effect of a given factor on the casting property is statistically significant. In essence, there’s less than a 5% chance the observed effect is due to randomness of experimental observations<sup>[33]</sup>. Statistical analysis results show that all three process parameters: filtration, runner thickness, and hydrogen content have statistically significant effects (*p*-value<0.05) on all four response variables within the experimental range examined. This confirms that controlling these casting variables would incredibly impact both the magnitude and consistency of the tensile properties of Al-Si alloy castings. The experimental findings were further

explored using a two-level full factorial design of experiments to quantify the influence of the significant casting parameters on the shape factor and characteristic life of ultimate tensile strength and percent elongation. The standardized effects and percentage contributions of all factors and interactions in this study are listed in Table 3. For a two-level factorial scheme, the effect of a factor is calculated as:

$$\text{Effect} = \text{Average response at high level} - \text{Average response at low level} \quad (2)$$

A positive sign is a suggestion of an improvement of the measured property when the factor level increases, and vice versa for negative effects. In addition, ANOVA decomposition quantifies the percentage contribution of each main effect and interaction to the total variation observed in the mechanical properties<sup>[36]</sup>. The percentage contribution is an absolute metric that quantifies the relative importance of each factor. It takes individual sum of squares (SS) for each parameter, normalized by the total sum of squares (SS<sub>total</sub>). This metric provides an objective ranking of process parameters based on their contribution to the variance in the responses, enabling the identification of the most influential variables for quality control and process optimization.

Factorial analysis identified strong parameter effect trends on all the mechanical property responses (Table 3). Hydrogen concentration exerted the most pronounced negative effects, with a doubling of its concentration reducing the UTS shape factor by 9.4 and characteristic life by 48 MPa, and

**Table 2: Area fraction of primary α-Al in Al-10Si modified with different amounts of Al-5Ti**

Source	Sum of squares	df	Mean square	F	p-value	R <sup>2</sup>
<b>Shape factor of UTS</b>						
Model	380	3	127	18	0.0090	0.93
A–Runner thickness (mm)	78	1	78	11	0.0300	
B–Filtration	127	1	127	18	0.0137	
C–Hydrogen content (cm <sup>3</sup> /100 g Al)	175	1	175	24	0.0078	
<b>Characteristic life of UTS (MPa)</b>						
Model	7,194	3	2,398	46	0.0015	0.97
A–Runner thickness (mm)	1,177	1	1,177	23	0.0089	
B–Filtration	1,339	1	1,339	26	0.0071	
C–Hydrogen content (cm <sup>3</sup> /100 g Al)	4,677	1	4,677	90	0.0007	
<b>Shape factor of elongation (%)</b>						
Model	82	3	27	42	0.0017	0.97
A–Runner thickness (mm)	12	1	12	18	0.0133	
B–Filtration	21	1	21	32	0.0048	
C–Hydrogen content (cm <sup>3</sup> /100 g Al)	50	1	50	77	0.0009	
<b>Characteristic life of elongation (%)</b>						
Model	29	3	10	24	0.0051	0.95
A–Runner thickness (mm)	6	1	6	14	0.0191	
B–Filtration	8	1	8	20	0.0108	
C–Hydrogen content (cm <sup>3</sup> /100 g Al)	15	1	15	37	0.0037	

Table 3: Full factorial analysis results

Term	Shape factor of UTS		Characteristic life of UTS (MPa)		Shape factor of elongation (%)		Characteristic life of elongation (%)	
	Effect	Contribution (%)	Effect	Contribution (%)	Effect	Contribution (%)	Effect	Contribution (%)
A - Runner thickness (mm)	-6.25	19.09	-24.26	15.91	-2.41	13.65	-1.71	19.06
B - Filtration	7.97	31.01	25.87	18.09	3.22	24.46	2.03	26.78
C - Hydrogen content (cm <sup>3</sup> /100 g Al)	-9.37	42.87	-48.36	63.20	-5.00	58.84	-2.74	48.88
AB	-0.35	0.06	-4.78	0.62	0.20	0.09	-0.32	0.67
AC	-0.26	0.03	6.24	1.05	-0.19	0.09	0.34	0.77
BC	-0.34	0.05	3.30	0.29	0.24	0.13	-0.66	2.83
ABC	-3.75	6.87	-5.56	0.84	-1.08	2.74	-0.39	1.00

elongation measurements by 5 units (shape factor) and 2.7% (characteristic life). Increasing the runner thickness exerts a parallel but weaker antagonistic effect, negatively impacting the four properties by 6.3, 24 MPa, 2.4, and 1.7%, respectively. In addition, filtration consistently improves every measured property and beneficial effects of about 8, 25.9 MPa, 3.2, and 2%, respectively. The ranked order was confirmed quantitatively using ANOVA results, which shows that hydrogen content dominates with an average contribution of 53%, followed by filtration (25%), and runner thickness (17%). Significantly, cross-factor effects are minimal, as evidenced by interaction effects between parameters accounting for an average of less than 5% of the observed variation. Quantitatively, under the optimized casting conditions (thin runner+melt filtration+low hydrogen), the UTS shape factor

increased by 474%, the elongation shape factor by 413%, the UTS characteristic life by 107%, and the elongation characteristic life by 149%, compared to the baseline condition (25 mm runner, no filter, high hydrogen).

These statistical conclusions are strongly supported by the results of microstructural examination, presented in Fig. 8. SEM analysis demonstrated the existence distinct oxide films at fracture surfaces of test bars from Experiments 1-3 and 5-7. Figures 8(a) and (b) showcase representative examples of these defects from Experiments 1 and 6, respectively. It can be seen, MgAl<sub>2</sub>O<sub>4</sub> (spinel) films are identified by energy dispersive X-ray. Conversely, specimens from Experiments 4 and 8 exhibit much cleaner fracture surface morphologies with no observable oxide films. This might be a suggestion that the defects are either too small to be detected at this level of

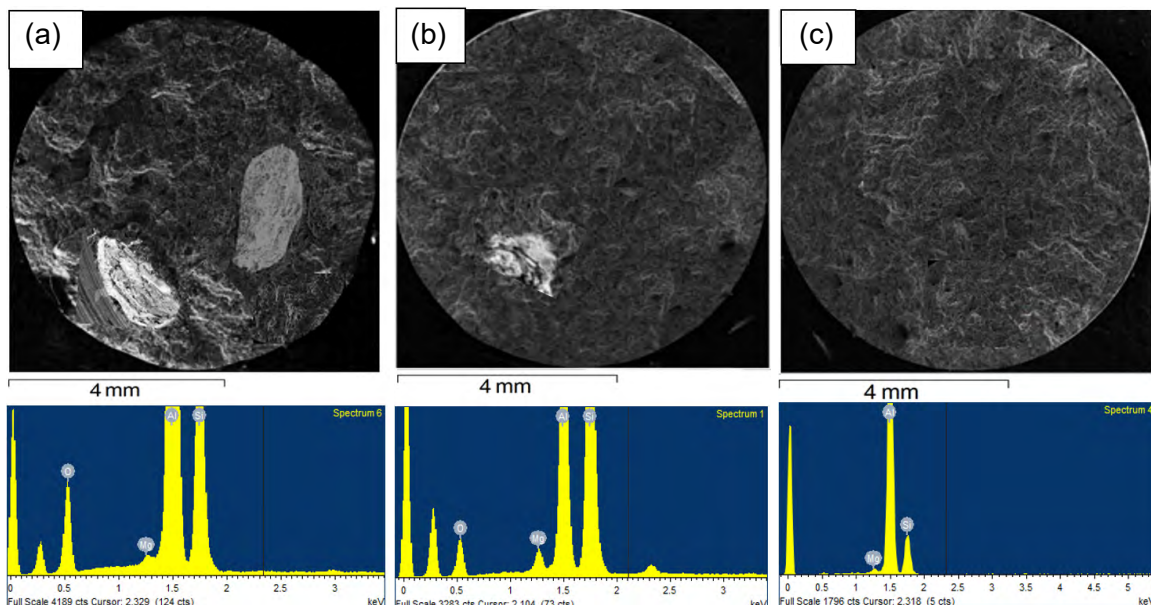


Fig. 8: SEM fractography of fracture surfaces from Experiment 1 (a), Experiment 6 (b), and Experiment 8 (c). EDX analysis carried out at marked locations “X”

SEM magnification or they have been eliminated from the Al casting. An example of a fracture surface from a sample from Experiment 8 is shown in Fig. 8(c).

Comparative fractography reveals evident morphological differences in oxide film entrainment among different experiments of varying casting conditions. Experiment 6 sample [Fig. 8(b)] exhibits noticeably smaller oxide fragments compared to the sample from Experiment 1 [Fig. 8(a)], and this size reduction is consistently observed across all low-hydrogen samples (Experiments 5–7) relative to their high-hydrogen counterparts (Experiments 1–3). The reduction in oxide size directly correlates with the decrease in dissolved hydrogen achieved through argon degassing, supporting the hypothesis that the dissolved hydrogen promotes oxide film growth during solidification. Most significantly, Experiment 8 fracture surfaces [Fig. 8(c)] exhibit no detectable oxide films, with EDX spectra indicating only aluminum, silicon, and magnesium peaks. This complete suppression of surface oxides is evidence of the synergistic effectiveness of thin runners (10 mm) combined with ceramic filtration in minimizing turbulent oxide entrainment during mold filling. Therefore, it could be argued that the statistical model's predictions were validated by this obvious correlation between the presence of oxide films and degradation of mechanical properties, showing how process variables govern defect formation, and, by extension, the final mechanical performance of the casting.

## 4 Discussion

The literature showed that inadequately controlled gating systems, particularly those featuring thick runners (25 mm) without filtration (Fig. 2), would generate excessive surface agitation upon mold filling, leading to significant oxide film entrainment<sup>[37]</sup>. These bifilms in entrainment severely degrade mechanical properties due to their non-bonded interfaces, as verified by Dispinar and Campbell<sup>[8]</sup>, Raiszadeh and Griffiths<sup>[38]</sup>, and later by El-Sayed et al<sup>[13]</sup>. Their collective efforts also showed that hydrogen contents in excess of the melt's solubility limit preferentially diffuse into the unbonded interfaces of bifilms, causing volumetric expansion that transforms these defects into hydrogen pores during solidification. This synergistic coupling of oxide entrapment and hydrogen uptake establishes a two-stage deterioration mechanism that significantly exacerbates casting defects and thereby worsen the mechanical properties. In the current research, 2L99 alloy melt was subjected to reduced-pressure (0.2 bar, 800 °C, 2 h) treatment to eliminate oxides existing in raw materials, so that the scatter of observed properties would solely result from the varying experimental conditions: runner thickness (10 or 25 mm), filtration (with or without 10 PPI ceramic filters), and hydrogen content (0.12 or 0.24 cm<sup>3</sup>/100g Al). Statistical analysis by means of DoE and ANOVA enabled a well-characterized understanding of bifilm behavior by decoupling the individual influence of these three significant casting parameters<sup>[13, 39]</sup>.

Within this framework, Experiment 1 was conducted using a poor gating system that was designed intentionally (25 mm runner with no filtration) along with high hydrogen content (0.24 cm<sup>3</sup>/100g Al) to provide a baseline for defect formation. The melt flow speed at the ingate was therefore expected to consistently exceed the critical threshold of 0.5 m·s<sup>-1</sup> ( $V_c$ ), promoting extensive oxide film entrainment, concurrently, elevated hydrogen concentrations further exacerbated defect formation by inflating bifilms into larger pores. Both mechanisms were verified by scanning electron microscopy [Fig. 8(a)]. These synergistic effects led to severe degradation of mechanical properties across all experiments, yielding a shortest characteristic life of 87 MPa for UTS and 4.1% for elongation, accompanied by high property scatter, as reflected by shape factors of 4.2 (UTS) and 2.3 (elongation). As corroborated by the data in Table 1 and Figs. 4 and 5, these conditions yielded the poorest mechanical properties, reflecting the detrimental impact of uncontrolled melt turbulence and high hydrogen content on cast quality.

Accordingly, statistical techniques through a full-factorial DoE and ANOVA were admitted to rigorously examine the impact of three significant casting parameters, runner thickness, filtration, and hydrogen content, on bifilm formation and mechanical properties of 2L99 alloy castings. As can be concluded from Tables 1 and 3, reducing the runner thickness from 25 mm to 10 mm and/or the application of filters bring about significant increases in shape factors and characteristic lives of ultimate tensile strength and elongation. Such gains reveal the importance of controlling the gating system design as a route for obtaining an optimum casting performance. The clear advancements of mechanical properties might be a consequence of inherent variations in melt flow dynamics. Narrowing the runner cross-section provides meniscus stability during mold filling, thereby restricting metal front disintegration, decreasing flow turbulence, and minimizing melt surface reoxidation. Strategic placement of ceramic filters simultaneously reduces flow acceleration, allowing a better-controlled filling pattern that maintains ingate flow velocities below the critical values for oxide entrainment. These suggestions were confirmed by scanning electron microscopy findings, which demonstrated substantially lower bifilm content in castings from Experiments 4 and 8 compared to baseline conditions, with an example presented in Fig. 8(c). Consequently, the castings from Experiments 4 and 8, where optimized gating system with filtration and thin runner was considered, offered substantial property improvements with average rise of 240% in UTS shape factor, 48% in UTS characteristic life, 173% in elongation shape factor, and 77% in elongation characteristic life compared to the unfiltered castings with 25 mm runners (Experiments 1 and 5), see Table 2. The microstructural observations are consistent with the obvious enhancement in mechanical properties, confirming the effectiveness of the combined process improvements. These findings supplement previous work by Green and Campbell<sup>[40, 41]</sup>, who achieved 350% improvement of shape factors through

turbulence-free filling systems of Al-7Si-Mg alloys. These findings also confirm the work carried by Bozchaloei et al.<sup>[42]</sup>, who also enhanced UTS and elongation reliability of aluminum castings using controlled mold filling techniques, demonstrating that ideal gating system design effectively guarantees mechanical property consistency in different applications of aluminum castings.

Finally, hydrogen content plays a crucial role in influencing the tensile properties of 2L99 Al-Si alloy castings. As listed in Table 3, the decrease of hydrogen content from 0.24 to 0.12 cm<sup>3</sup>/100 g Al significantly improves the shape factors and characteristic lives of both ultimate tensile strength and elongation. This hydrogen-dependent trend was microstructurally supported by comparative fractographic analysis [Figs. 12(a), (b)], in which notably smaller oxide films were observed in low-hydrogen samples (Experiment 6) than in their high-hydrogen counterparts (Experiment 1). The larger defect size in castings from the latter experiment suggests hydrogen-mediated inflation of bifilms, which promoted crack initiation and propagation, ultimately leading to a deterioration in mechanical performance. The mechanical property improvements achieved through hydrogen control were dramatic, with low-hydrogen castings (Experiments 5–8) showing 132% average increases in the UTS and 128% in elongation shape factors, and corresponding average increases of 47% and 54%, respectively in characteristic lives. These findings complement and extend earlier investigations by El-Sayed and Griffiths<sup>[37]</sup>, who obtained even more astonishing property enhancements (400% in UTS and 200% elongation shape factors) when reducing hydrogen content from 0.18 to 0.08 cm<sup>3</sup>/100 g Al in the same aluminum alloy system. The concordant trends in investigations had likewise identified hydrogen content as a significant control parameter for optimizing performance of aluminum casting.

These findings demonstrate that the strategic runner system optimization in this work, through reduced runner thickness and adding filtration, can be highly effective in preventing oxide film formation during mold filling. Meanwhile, low hydrogen levels provided by appropriate melt and mold treatments would decrease the amount of hydrogen diffusing into entrained bifilms and the eventual bifilm growth into larger defects. The combined application of these practices enables a dramatic improvement in casting quality to be achieved through a proper dominance of both defect initiation and growth mechanisms. Practical implementation of these findings enables a dual-path optimization of the casting process: (1) adoption of effective melt treatment practices involving melt degassing and extended mold vacuuming to reduce the hydrogen content in the Al castings, and (2) employment of optimized gating systems with thin runners and ceramic foam filters. Through this two-fold approach, both quiescent mold filling and limited bifilm expansion could be achieved, collectively resulting in Al castings with enhanced and more consistent mechanical properties. Such process controls enable foundries to possess a good technique of producing high-integrity cast components with reliable and reproducible performance.

## 5 Conclusions

The present study systematically investigated the effect of runner thickness, filtration, and hydrogen content on the mechanical properties of Al-Si (2L99) cast alloys using a 2<sup>3</sup> full factorial design of experiments. The main findings are summarized below:

(1) Hydrogen content is identified as the most critical factor, accounting for about 53% of the property variation. Reducing hydrogen concentration from 0.24 to 0.12 cm<sup>3</sup>/100 g Al significantly improved the shape factors and characteristic lives of both UTS and elongation by limiting bifilm inflation into porosity.

(2) Filtration (using a 10 PPI ceramic filter) and reducing runner thickness from 25 mm to 10 mm also play a significant role, accounting for about 25% and 17%, respectively, to the variation in mechanical properties. Their synergistic effect promotes stable melt flow, minimizes oxide entrainment, and enhances mechanical consistency.

(3) Optimized process conditions (thin runner, filtration, and low hydrogen) resulted in maximum improvements of the UTS shape factor, elongation shape factor, UTS characteristic life, and elongation characteristic life by about 470%, 410%, 110%, and 150%, respectively. SEM fractography confirmed near-complete elimination of bifilm defects under these conditions, which was consistent with the peak mechanical properties obtained.

Overall, the results highlight that careful control of melt treatment and gating system design is essential to minimize defects while enhancing strength, ductility, and reliability of Al-Si alloy castings, thereby establishing a foundation for producing high-integrity Al cast alloys.

## Acknowledgment

This work was supported and funded by the Deanship of Scientific Research at Imam Mohammad Ibn Saud Islamic University (IMSIU) (Grant number IMSIU- DDRSP2603).

## Conflict of interest

The authors declare that they have no conflict of interest.

## References

- [1] Campbell J. Castings, 2nd Edition, Butterworth-Heinemann, 2003.
- [2] Weigel J and Fromm E. Determination of hydrogen absorption and desorption processes in aluminum melts by continuous hydrogen activity measurements. *Metallurgical Transactions: B*, 1990, 21: 855–860.
- [3] Hassanin H, Ahmed El-Sayed M, ElShaer A, et al. Microfabrication of net shape zirconia/alumina nanocomposite micro parts. *Nanomaterials*, 2018, 8: 593.
- [4] Olofsson J, Bogdanoff T, Tiryakioğlu M, et al. The effect of hidden damage on local process variability in Al-10 Pct Si alloy high-pressure die castings. *Metallurgical and Materials Transactions: B*, 2024: 1–13.

- [5] Gyarmati G, Bubonyi T, Fegyverneki G, et al. Interactions of primary intermetallic compound particles and double oxide films in liquid aluminum alloys. *Intermetallics*, 2022, 149, 107681.
- [6] Scampone G, Pirovano R, Mascetti S, et al. Experimental and numerical investigations of oxide-related defects in Al alloy gravity die castings. *The International Journal of Advanced Manufacturing Technology*, 2021, 117: 1765–1780.
- [7] Gyarmati G, Vincze F, Fegyverneki G, et al. The effect of rotary degassing treatments with different purging gases on the double oxide- and nitride film content of liquid aluminum alloys. *Metallurgical and Materials Transactions: B*, 2022, 53: 1244–1257.
- [8] Dispinar D, and Campbell J. Critical assessment of reduced pressure test. Part 1: Porosity phenomena. *International Journal of Cast Metals Research*, 2004, 17: 280–286.
- [9] El-Sayed M, Hassanin H, and Essa K. Effect of casting practice on the reliability of Al cast alloys. *International Journal of Cast Metals Research*, 2016, 29: 350–354.
- [10] Griffiths W D, Caden A, and El-Sayed M. An investigation into double oxide film defects in aluminium alloys. In *Materials Science Forum*, 2014, 783: 142–147.
- [11] Chen Q, and Griffiths W D. The investigation of the floatation of double oxide film defect in liquid aluminium alloys by a four-point bend test. *International Journal of Cast Metals Research*, 2019, 32: 221–228.
- [12] Chen Q, and Griffiths W D. Modification of double oxide film defects with the addition of Mo to an Al-Si-Mg alloy. *Metallurgical and Materials Transactions: B*, 2021, 52: 502–516.
- [13] El-Sayed M A. A study of the behaviour of double oxide films in Al alloy melts. In: 6th International Light Metals Technology Conference, LMT 2013, Old Windsor, United Kingdom.
- [14] Campbell J. Entrainment defects. *Materials Science and Technology*, 2006, 22: 127–145.
- [15] Olofsson J, Bogdanoff T, and Tiryakioğlu M. On revealing hidden entrainment damage during in situ tensile testing of cast aluminum alloy components. *Materials Characterization*, 2024, 208, 113647.
- [16] Runyoro J, Boutorabi S M A, and Campbell J. Critical gate velocities for film-forming casting alloys: A basic for process specification. *AFS Transactions*, 1992, 100: 225–234.
- [17] Halvae A, and Campbell J. Critical mold entry velocity for aluminum bronze castings. *AFS Transactions*, 1997, 105: 35–46.
- [18] Bahreinian F, Boutorabi S M A, and Campbell J. Critical gate velocity for magnesium casting alloy (ZK51A). *International Journal of Cast Metals Research*, 2006, 19: 45–51.
- [19] Bruna M, and Galčík M. Effect of filter type on mechanical properties during aluminium alloy casting. *Archives of Foundry Engineering*, 2022, 22: 95–98.
- [20] Brúna M, Galčík M, Pastircak R, et al. Effect of gating system design on the quality of aluminum alloy castings. *Metals*, 2024, 14: 312.
- [21] Esim O, Savaser A, Ozkan C K, et al. Effect of polymer type on characteristics of buccal tablets using factorial design. *Saudi Pharmaceutical Journal*, 2018, 26: 53–63.
- [22] Hassanin H, El-Sayed M A, Ahmadein M, et al. Optimising surface roughness and density in titanium fabrication via laser powder bed fusion. *Micromachines*, 2023, 14: 1642.
- [23] Naveen N R, Gopinath C, and Rao D S. Design expert supported mathematical optimization of repaglinide gastroretentive floating tablets: In vitro and in vivo evaluation. *Future Journal of Pharmaceutical Sciences*, 2017, 3: 140–147.
- [24] Verma D, Thakur P S, Padhi S, et al. Design expert assisted nanoformulation design for co-delivery of topotecan and thymoquinone: Optimization, in vitro characterization and stability assessment. *Journal of Molecular Liquids*, 2017, 242: 382–394.
- [25] Sequeira S. Factorial design. In: *Translational orthopedics* (Elsevier), Edited by Adam E M E, Jeffrey A B, Jack M H, et al. Academic Press, 2024: 261–263. <https://doi.org/10.1016/C2020-0-02793-3>
- [26] Djuris J, Vasiljevic D, and Ibric S. Experimental design application and interpretation in pharmaceutical technology. In: *Computer-aided applications in pharmaceutical technology* (Elsevier), Woodhead Publishing Series in Biomedicine, 2024: 61–85. <https://doi.org/10.1533/9781908818324.31>
- [27] Ginocchi M, Penthong T, Ponci F, et al. Statistical design of experiments for power system protection testing: A case study for distance relay performance testing. *IEEE Access*, 2024, 12: 27052–27072.
- [28] Croarkin C, Tobias P, and Zey C. *Engineering statistics handbook*, Chapter 2: Measurement process characterization. 2002, (NIST iTL).
- [29] El-Sayed M, and Griffiths W. Hydrogen, bifilms and mechanical properties of Al castings. *International Journal of Cast Metals Research*, 2014, 27: 282–287.
- [30] Winardi L, Griffin R D, Littleton H E, et al. Variables affecting gas evolution rates and volumes from cores in contact with molten metal. *Transactions of the American Foundrymen's Society*, 2008, 116: 505–521.
- [31] Nyahumwa C, Green N R, and Campbell J. The concept of the fatigue potential of cast alloys. *Journal of the Mechanical Behavior of Materials*, 1998, 9: 227–236.
- [32] Basuny F H, Ghazy M, Kandeil A R Y, et al. Effect of casting conditions on the fracture strength of Al-5 Mg alloy castings. *Advances in Materials Science and Engineering*, 2016, 6496348.
- [33] Akinwande A A, Adediran A A, Balogun O A, et al. Optimization of selected casting parameters on the mechanical behaviour of Al 6061/glass powder composites. *Heliyon*, 2022, 8. <https://doi.org/10.1016/j.heliyon.2022.e09350>
- [34] Weibull W. A statistical distribution function of wide applicability. *Journal of Applied Mechanics*, 1951, 13: 293–297.
- [35] Nayak A K, Pal D, and Santra K. Ispaghula mucilage-gellan mucoadhesive beads of metformin HCl: Development by response surface methodology. *Carbohydrate Polymers*, 2014, 107: 41–50.
- [36] El-Sayed M A, and Griffiths W D. Hydrogen, bifilms and mechanical properties of Al castings. *International Journal of Cast Metals Research*, 2014, 27: 282–287.
- [37] Raiszadeh R, and Griffiths W D. A method to study the history of a double oxide film defect in liquid aluminum alloys. *Metallurgical and Materials Transactions: B*, 2006, 37: 865–871.
- [38] El-Sayed M, Hassanin H, and Essa K. Effect of casting practice on the reliability of Al cast alloys. *International Journal of Cast Metals Research*, 2016, 29: 350–354.
- [39] El-Sayed M, Hassanin H, and Essa K. Bifilm defects and porosity in Al cast alloys. *The International Journal of Advanced Manufacturing Technology*, 2016, 86: 1173–1179.
- [40] Green N, and Campbell J. Influence of oxide film filling defects on the strength of Al-7Si-Mg alloy castings. *Transactions of the American Foundrymen's Society*, 1994, 102: 341–348.
- [41] Green N R, and Campbell J. Statistical distributions of fracture strengths of cast Al-7Si-Mg alloy. *Materials Science and Engineering: A*, 1993, 173: 261–266.
- [42] Bozchaloei G E, Varahram N, Davami P, et al. Effect of oxide bifilms on the mechanical properties of cast Al-7Si-0.3 Mg alloy and the roll of runner height after filter on their formation. *Materials Science and Engineering: A*, 2012, 548: 99–105.